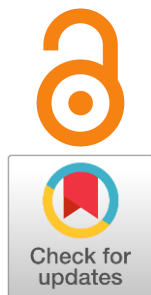


## Composite solid electrolytes based on $\text{Li}_7\text{La}_3\text{Zr}_2\text{O}_{12}$ for all-solid-state lithium power sources

Evgeniya Il'ina<sup>a,\*</sup>Received: 3 June 2024  
Accepted: 22 June 2024  
Published online: 27 June 2024DOI: [10.15826/elmattech.2024.3.038](https://doi.org/10.15826/elmattech.2024.3.038)

Currently development of all-solid-state lithium batteries are in great demand all over the world.  $\text{Li}_7\text{La}_3\text{Zr}_2\text{O}_{12}$  (LLZ) compounds are considered as perspective solid electrolyte for such power sources. However, these solid electrolytes of garnet family have some disadvantages – high temperatures of ceramic synthesis, poor wettability by Li and low stability to air components. The creation of composite solid electrolytes based on LLZ is one of the ways to solve these problems. It was established that the temperature and/or sintering time of the solid electrolyte could be reduced by the introduction of different additives with maintaining lithium-ion conductivity values ( $10^{-5}$ – $10^{-4}$  S/cm at room temperature). It should be noted that the used sintering additive should meet the following requirements: low softening temperatures, high values of lithium-ion conductivity, stability in contact with lithium metal and absence of chemical interaction between components leading to the formation of low-conductivity impurity phases. Thus, the development of composite solid electrolytes based on LLZ is perspective for all-solid-state power sources.

**keywords:** composite solid electrolyte, sintering additive, glass, lithium-ion conductivity, lithium anode, all-solid-state battery

© 2024, the Authors. This article is published in open access under the terms and conditions of the Creative Commons Attribution (CC BY) license (<http://creativecommons.org/licenses/by/4.0/>).

### 1. Introduction

Currently, the development of all-solid-state power sources is under great demand all over the world [1–5]. During the operation of traditional lithium-ion batteries with a liquid (or polymer, gel) electrolyte, the dendrite formation and gas evolution are possible, which lead to rapid degradation of the device and limit the battery life. Thus, the transition to the all-solid-state design is positioned as a possible way to solve the safety problem (especially in extreme operating conditions – elevated temperatures, pressure and aggressive environments) and increase the service life of the power source. It is worth noting that the safety problem becomes especially acute as the battery size increases. If modern portable batteries, despite the use of liquid electrolytes, are practically not prone to gas formation and swelling, then in their larger counterparts, heating of the electrolytes, their boiling and

even explosions are far from rare. Moreover, the transition from liquid to solid electrolytes allows considering metallic lithium as an anode material. Li has record energy intensity values – high theoretical specific capacity (3860 mA · h/g), low electrode potential (–3.040 V vs SHE), and low density (0.59 g/cm<sup>3</sup>).

$\text{Li}_7\text{La}_3\text{Zr}_2\text{O}_{12}$  (LLZ) compounds with a garnet-based structure are considered as promising solid electrolytes for all-solid-state lithium power sources [6–8]. After intensively studying the influence of various dopants on the structure and conductivity of solid electrolytes based on LLZ [9–11], since 2013, researchers have turned their attention to studying the influence of sintering additives, including glasses, on the properties of the solid electrolyte. The conductivity and density of ceramic materials can be increased by introducing sintering additives, for example, lithium salts or by preparing glass-ceramic composites. It is worth noting that inorganic glasses are capable of filling the pores of ceramic materials; they have good thermal and mechanical characteristics, as well as high values of lithium-ion conductivity. In addition, in the studies presented in the literature

a: Laboratory of Chemical Power Sources, Institute of High-temperature electrochemistry, Yekaterinburg 620066, Russia

\* Corresponding author: [ilvina@ihste.ru](mailto:ilvina@ihste.ru)

[9, 12, 13] the temperature and/or sintering time of the ceramic LLZ was reduced by the introduction of different additives such as  $\text{Li}_3\text{BO}_3$ ,  $\text{Li}_3\text{PO}_4$ ,  $\text{Li}_4\text{SiO}_4$  or lithium containing multicomponent glasses, and conductivity values of solid electrolytes were maintained at the level of  $10^{-5}$ – $10^{-4}$  S/cm at 30 °C.

The creation of a dense and highly conductive interface between lithium metal and the LLZ-based solid electrolyte is one of the main challenges for the successful implementation of high-energy all-solid-state power sources. Moreover, there is a number of problems that arise during the formation and cycling of electrochemical cells based on the solid electrolyte with Li anode [14–18]:

- growth of Li dendrites through the solid electrolyte, leading to a short circuit;

- poor wettability of the solid electrolyte surface with lithium metal, leading to the formation of voids (pores) at the interface between two phases.

According to the literature data [6, 9, 11], one of the way to solve these problems may be transition to the composite electrolyte containing a mixture of solid electrolyte components with functional materials to obtain a high-density ceramic membrane, improve contact with Li anode and suppress the growth of Li dendrites at grain boundaries.

Another advantage of composite electrolytes based on LLZ is their improved stability towards environmental components (water,  $\text{CO}_2$ ) [6, 9]. Since, according to literature data, solid electrolytes of the LLZ family are prone to increased degradation of the ceramic surface due to interaction with air components [19–21].

The aim of this review was to analyze the data available in the literature on the effect of various lithium-conducting sintering additives on the heat treatment mode, conductivity, and density of solid electrolytes with a garnet-like structure, as well as their stability in contact with air components and suppression of lithium dendrite formation.

### 1.1. Effect of various sintering additives on the conductivity of LLZ

Various sintering additives to LLZ ceramics have different effects on the morphology, density, and phase composition of their composites, which, in turn, affects the transport properties of solid electrolytes. The action mechanism of different sintering additives on the electrolyte conductivity depends from their nature. Some sintering additives are located at grain boundaries; the other can incorporate into grains of solid electrolytes based on LLZ. Therefore, in the first case, the grain-boundary conductivity increases; in the second, the sintering additive can also improve the bulk conductivity.

More often, sintering additives of the first group are used for LLZ composites.  $\text{Al}_2\text{O}_3$  is one of the sintering additives, which can incorporate into LLZ grains. Moreover, at high annealing temperatures [13] it can form a lithium-conductive liquid phase with lithium oxide from LLZ.

Basappa RH et al. [22] used 2 wt. % LiOH addition to  $\text{Li}_{6.5}\text{La}_3\text{Zr}_{1.5}\text{Ta}_{0.5}\text{O}_{12}$  solid electrolyte. Due to the low melting points of LiOH (462 °C), the additive melts and fills the voids during heat treatment at 900 °C for 12 h. Such modification of ceramic grain boundaries leads to the growth of the conductivity of the samples up to  $7.6 \cdot 10^{-4}$  S/cm. Hao S et al. [23] improved Li-ion motion along  $\text{Li}_{6.25}\text{La}_3\text{Zr}_2\text{Al}_{0.25}\text{O}_{12}$  grains by introducing 3 wt. % LiBr. Such a modification leads to conductivity growth from  $1.1 \cdot 10^{-4}$  to  $2.8 \cdot 10^{-4}$  S/cm. The electrochemical cell with Li anode,  $\text{LiCoO}_2$  cathode and composite electrolyte showed cyclic stability and capacity retention. However, the sintering temperature and time are still remained high (900 °C for 6 h, 1100 °C for 6 h, and 1200 °C for 12 h). The anti-perovskite of  $\text{Li}_3\text{OCl}$  electrolyte was used as sintering additive to  $\text{Li}_{6.75}\text{La}_3\text{Zr}_{1.75}\text{Ta}_{0.25}\text{O}_{12}$  [24]. A composite electrolyte with the amorphous  $\text{Li}_3\text{OCl}$  with high ionic conductivity ( $2.27 \cdot 10^{-4}$  S/cm) was obtained at 350 °C.

However,  $\text{Li}_3\text{BO}_3$  is most often used as a sintering additive introduced into LLZ-based solid electrolytes. This compound has a low melting point (700 °C) and fairly high lithium-ion conductivity values ( $\sim 10^{-6}$  S/cm at 25 °C) [25]. For example, Shin RN et al. [26] studied the mechanism of cubic LLZ – 8 wt. %  $\text{Li}_3\text{BO}_3$  composite sintering. It was established that the process of sintering is caused by viscous glass flow at low temperatures and leads to ceramic densification. The lithium-ion conductivity of the obtained composite after annealing at 1100 °C for 8 h was equal to  $1.94 \cdot 10^{-5}$  S/cm at room temperature. Takano R [27] and Rosero-Navarro NC [28] reduced the annealing temperature of composite solid electrolytes with the addition of  $\text{Li}_3\text{BO}_3$  to 900 °C (10 h). Cubic LLZ stabilized by Al after annealing at 900 °C has low values of conductivity –  $1.6 \cdot 10^{-6}$  S/cm, but  $\text{Li}_3\text{BO}_3$  addition leads to conductivity growth by an order of magnitude ( $1.9 \cdot 10^{-5}$  S/cm) [27]. The introduction of 6.5 wt. %  $\text{Li}_3\text{BO}_3$  to  $\text{Li}_7\text{La}_3\text{Zr}_{1.75}\text{Nb}_{0.25}\text{O}_{12}$  leads to density and lithium-ion conductivity growth up to 90 % and  $7 \cdot 10^{-5}$  S/cm at 30 °C, respectively; which is two orders of magnitude higher compared to the initial electrolyte [28]. Moreover, it was found that composite solid electrolytes with  $\text{LiBO}_2$  additive have low-conductive impurity phase of  $\text{La}_2\text{Zr}_2\text{O}_7$ . In the work Tadanaga K et al. [29] higher conductivity values for composite solid electrolyte with  $\text{Li}_3\text{BO}_3$  additive were achieved ( $1 \cdot 10^{-4}$  S/cm at 30 °C) after the introduction of lithium borate in the molar ratio  $\text{Li}_3\text{BO}_3/\text{LLZ}$  (0.68) and subsequent annealing at 900 °C

during 36 h.  $\text{Li}_3\text{BO}_3$  was also used as sintering additive for thick sheets of solid electrolyte based on  $\text{Li}_7\text{La}_3\text{Zr}_{1.75}\text{Nb}_{0.25}\text{Al}_{0.1}\text{O}_{12}$  with a thickness of 150  $\mu\text{m}$  by Jonson RA and McGinn PJ [30]. It was found that for bulk samples the optimal additive content was equal to 1–2 wt. %  $\text{Li}_3\text{BO}_3$  ( $\sim 2.5 \cdot 10^{-4}$  S/cm), while for thick sheets of the solid electrolyte obtained by tape casting a lower additive content was required – 0.5 wt. %  $\text{Li}_3\text{BO}_3$  ( $2.83 \cdot 10^{-4}$  S/cm). The obtained composite electrolytes were sintered at 1000 °C for 6 h in an Ar.

Zhao G et al. [31] used the boron nitride (BN) as a sintering additive. During sintering, BN interacts with  $\text{Li}_2\text{CO}_3$  present on the surface of  $\text{Li}_{6.25}\text{Ga}_{0.25}\text{La}_3\text{Zr}_2\text{O}_{12}$  (LGLZO) grains to form the  $\text{Li}_3\text{BO}_3$  phase (Figure 1). This effect leads to an increase in the density of the solid electrolyte (up to 93 %), mechanical strength (up to 5.36 GPa) and lithium-ion conductivity ( $6.7 \cdot 10^{-4}$  S/cm). In [32], the  $\text{Li}_{2.3}\text{Co}_{0.7}\text{B}_{0.3}\text{O}_3$  compound was chosen as a sintering additive due to its low melting point (700 °C), stability in contact with lithium metal and acceptable conductivity values ( $10^{-6}$ – $10^{-7}$  S/cm). The composite electrolyte based on LLZ after annealing at 1000 °C for 15 h had high values of lithium-ion conductivity ( $1 \cdot 10^{-4}$  S/cm).

Since the conductivity of  $\text{Li}_3\text{BO}_3$  is significantly lower than cubic LLZ and a large amount of additive can lead to a decrease in the conductivity of the composite, then the effect of the simultaneous introduction of two additives in cubic LLZ was investigated [33–36]. These two additives play different roles – one leads to a modification of the bulk of ceramic grains, the second exists at the grain boundaries. For example, the effect of  $\text{Al}_2\text{O}_3$  and  $\text{Li}_3\text{BO}_3$  introduction in  $\text{Li}_{7-x}\text{La}_{2.95}\text{Ca}_{0.05}\text{ZrTaO}_{12}$  was studied in work [33]. The addition of 0.21 mol of  $\text{Al}_2\text{O}_3$  and 0.80 mol of  $\text{Li}_3\text{BO}_3$  followed by annealing at 900 °C for 10 h leads to the formation of a composite electrolyte with a relative density of 95 % and a lithium-ion conductivity

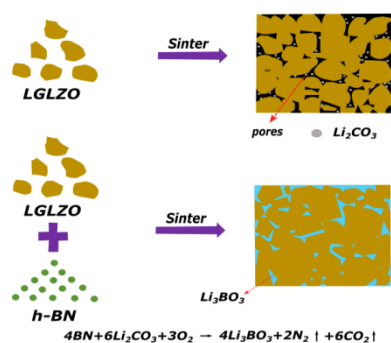


**Figure 1** Schematic describing the role of BN additive in optimizing  $\text{Li}_{6.25}\text{Ga}_{0.25}\text{La}_3\text{Zr}_2\text{O}_{12}$  solid electrolyte grain boundaries.

of  $1 \cdot 10^{-4}$  S/cm at 32 °C. L.C. Zhang et al. [34] prepared a composite solid electrolyte based on Ta- and Ca-doped LLZ ( $\text{Li}_{6.55}\text{La}_{2.95}\text{Ca}_{0.05}\text{Zr}_{1.5}\text{Ta}_{0.5}\text{O}_{12}$ ) using the same sintering additives with a subsequent heat treatment at 800 °C for 20 h. It has been shown that at a molar ratio of  $\text{Li}_3\text{BO}_3$  to solid electrolyte equal to 80 %, an increase in conductivity was observed from  $2.83 \cdot 10^{-6}$  (without additive) to  $1.33 \cdot 10^{-4}$  S/cm at 30 °C. In work [35], low-temperature sintering of  $\text{Li}_{6.5}\text{La}_{2.925}\text{Ca}_{0.075}\text{Zr}_{1.425}\text{Sb}_{0.575}\text{O}_{12}$  at 750 °C was achieved using low-melting additives –  $\text{Li}_7\text{SbO}_6$  and  $\text{Li}_3\text{BO}_3$ . The conductivity of the obtained composite electrolyte with the optimal content of additives was equal to  $3.1 \cdot 10^{-4}$  S/cm at room temperature with a relative density of the electrolyte membrane of 87 %.

Rosero-Navarro NC et al. [36] also used two additives (75  $\text{Li}_2\text{O} \cdot 25 \text{B}_2\text{O}_3$  and aluminum oxide) to create a composite electrolyte based on Ta-doped LLZ (LLZT). A distinctive feature of this work was the use of precursors of  $\text{Li}_2\text{O}-\text{B}_2\text{O}_3$  (LBO) and  $\text{Al}_2\text{O}_3$  sintering additives, obtained in the form of a sol, followed by mixing with a solid electrolyte and annealing at 1000 °C. The obtained composite with 0.5 wt. % LBO and 1.2 mol %  $\text{Al}_2\text{O}_3$  had high conductivity values of 0.8 mS/cm at 25 °C. Figure 2 shows an illustration reflecting the process of liquid-phase sintering using powder sintering additives and their precursors prepared in the form of a solution (sol). It should be noted that the obtained composite electrolytes possess the highest values of lithium-ion conductivity among the observed composites due to the proposed technique.

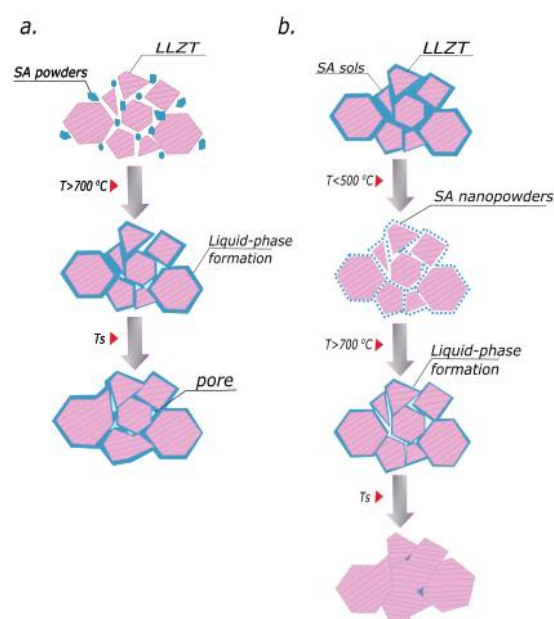


**Figure 2** Illustration of liquid-phase sintering using powder (a) and sintering additives obtained in solution (b).

Besides lithium borate,  $\text{Li}_3\text{PO}_4$  and  $\text{Li}_4\text{SiO}_4$  glasses were considered as sintering additives [37–41]. It was established that it is possible to reduce the sintering time of the ceramic membrane from 36 to 6 h at 1175 °C by adding 1–6 wt. %  $\text{Li}_3\text{PO}_4$  glass in  $\text{Li}_{6.75}\text{La}_3\text{Zr}_{1.75}\text{Ta}_{0.25}\text{O}_{12}$  solid electrolyte. The composite solid electrolyte with 1 wt. %  $\text{Li}_3\text{PO}_4$  had high values of lithium-ion conductivity –  $7.2 \cdot 10^{-4}$  S/cm [37]. In [38],  $\text{Li}_{6.5}\text{La}_3\text{Zr}_{1.5}\text{Ta}_{0.5}\text{O}_{12}$  with the addition of 2 wt. %  $\text{Li}_3\text{PO}_4$  had lower conductivity values ( $1.4 \cdot 10^{-4}$  S/cm) compared to the solid electrolyte without additive –  $4.6 \cdot 10^{-4}$  S/cm. Moreover, Pershina SV et al. [39] investigated the influence of  $\text{Li}_3\text{PO}_4$  glass addition on the conductivity of Al-doped LLZ. The composite electrolyte with 1 wt. % addition sintered at 1150 °C for 1 h possessed the highest lithium ion conductivity –  $1.1 \cdot 10^{-4}$  S/cm. The ionic

conductivities of the composites decreased with the rise of the  $\text{LiPO}_3$  glass content, because of the low-conductivity phase (crystalline  $\text{Li}_3\text{PO}_4$ ) formation.

In [40], 1 wt. %  $\text{Li}_4\text{SiO}_4$  was added to the solid electrolyte  $\text{Li}_{6.16}\text{Al}_{0.28}\text{La}_3\text{Zr}_2\text{O}_{12}$ . The addition of  $\text{Li}_4\text{SiO}_4$  glass and heat treatment at 1200 °C lead to the formation of composite solid electrolyte with a total conductivity of  $6.1 \cdot 10^{-4}$  S/cm at 33 °C and a relative density of 96 %. Patra S et al. [41] also used 1 wt. %  $\text{Li}_4\text{SiO}_4$  additive to the  $\text{Li}_{6.16}\text{Al}_{0.28}\text{La}_3\text{Zr}_2\text{O}_{12}$  solid electrolyte. A composite solid electrolyte obtained by hot pressing (1158 °C for 2 min, 127 MPa) possesses high values of lithium-ion conductivity – 0.41 mS/cm at room temperature. It was found that during hot pressing the additive remains in a glassy state and fills all voids (Figure 3).

**Table 1** – Composite solid electrolytes based on LLZ.

Solid electrolyte	Additive	$\sigma_t$ at RT, S/cm	$\rho$ , %	Heat treatment mode	Ref.
$\text{Li}_{6.5}\text{La}_3\text{Zr}_{1.5}\text{Ta}_{0.5}\text{O}_{12}$	2 wt. % LiOH	$7.6 \cdot 10^{-4}$	96.4	900 °C, 12 h	[22]
$\text{Li}_{6.25}\text{La}_3\text{Zr}_2\text{Al}_{0.25}\text{O}_{12}$	3 wt. % LiBr	$2.8 \cdot 10^{-4}$	89.2	1200 °C, 12 h	[23]
$\text{Li}_{6.75}\text{La}_3\text{Zr}_{1.75}\text{Ta}_{0.25}\text{O}_{12}$	2 wt. % $\text{Li}_3\text{OCl}$	$2.27 \cdot 10^{-4}$	94.0	350 °C, 12 h	[24]
Commercial LLZ (cubic)	8 wt. % $\text{Li}_3\text{BO}_3$	$1.94 \cdot 10^{-5}$	86.4	1100 °C, 8 h	[26]
Al-doped $\text{Li}_7\text{La}_3\text{Zr}_2\text{O}_{12}$	$\text{Li}_3\text{BO}_3$ ( $\chi = 0.68$ )	$1.9 \cdot 10^{-5}$	–	900 °C, 10 h	[27]
$\text{Li}_7\text{La}_3\text{Zr}_{1.75}\text{Nb}_{0.25}\text{O}_{12}$	6.5 wt. % $\text{Li}_3\text{BO}_3$	$7.0 \cdot 10^{-5}$	86.0	900 °C, 10 h	[28]
Al-doped $\text{Li}_7\text{La}_3\text{Zr}_2\text{O}_{12}$	$\text{Li}_3\text{BO}_3$	$1.0 \cdot 10^{-4}$	92.0	900 °C, 36 h	[29]
$\text{Li}_7\text{La}_3\text{Zr}_{1.75}\text{Nb}_{0.25}\text{Al}_{0.1}\text{O}_{12}$	1–2 wt. % $\text{Li}_3\text{BO}_3$	$2.5 \cdot 10^{-4}$	83.5	1000 °C, 6 h	[30]
$\text{Li}_7\text{La}_3\text{Zr}_{1.75}\text{Nb}_{0.25}\text{Al}_{0.1}\text{O}_{12}$	0.5 wt. % $\text{Li}_3\text{BO}_3$	$2.83 \cdot 10^{-4}$	90.0	tape-casting, 1000 °C, 6 h	[30]
$\text{Li}_{6.25}\text{Ga}_{0.25}\text{La}_3\text{Zr}_2\text{O}_{12}$	2 mol % BN	$6.7 \cdot 10^{-4}$	92.9	1150 °C, 6 h	[31]
$\text{Li}_{6.55}\text{La}_3\text{Zr}_{1.55}\text{Ta}_{0.45}\text{O}_{12}$	8.9 wt. % $\text{Li}_{2.3}\text{Co}_7\text{B}_{0.3}\text{O}_3$	$1.0 \cdot 10^{-4}$	88.0	1000 °C, 15 h	[32]
$\text{Li}_{7-x}\text{La}_{2.95}\text{Ca}_{0.05}\text{ZrTaO}_{12}$	0.21 mol $\text{Al}_2\text{O}_3$ , 0.80 mol $\text{Li}_3\text{BO}_3$	$1.0 \cdot 10^{-4}$	95.0	900 °C, 10 h	[33]
$\text{Li}_{6.55}(\text{La}_{2.95}\text{Ca}_{0.05})(\text{Zr}_{1.5}\text{Ta}_{0.5})\text{O}_{12}$	80 mol % $\text{Li}_3\text{BO}_3$ : LLZ	$1.33 \cdot 10^{-4}$	–	800 °C, 20 h	[34]
$\text{Li}_{6.5}(\text{La}_{2.925}\text{Ca}_{0.075})(\text{Zr}_{1.425}\text{Sb}_{0.575})\text{O}_{12}$	0.08 $\text{Li}_7\text{SbO}_6$ , $\text{Li}_3\text{BO}_3$ (4.75 : 1)	$3.1 \cdot 10^{-4}$	87.0	750 °C, 24 h	[35]
Ta-doped $\text{Li}_7\text{La}_3\text{Zr}_2\text{O}_{12}$	0.5 wt. % LBO and 1.2 mol % $\text{Al}_2\text{O}_3$	$8.0 \cdot 10^{-4}$	88.0	1000 °C	[36]
$\text{Li}_{6.75}\text{La}_3\text{Zr}_{1.75}\text{Ta}_{0.25}\text{O}_{12}$	1 wt. % $\text{Li}_3\text{PO}_4$	$7.2 \cdot 10^{-4}$	92.7	1175 °C, 6 h	[37]
$\text{Li}_{6.5}\text{La}_3\text{Zr}_{1.5}\text{Ta}_{0.5}\text{O}_{12}$	5 wt. % $\text{Li}_3\text{PO}_4$	$1.4 \cdot 10^{-4}$	–	1140 °C, 16 h	[38]
Al-doped $\text{Li}_7\text{La}_3\text{Zr}_2\text{O}_{12}$	$\text{Li}_3\text{PO}_4$	$1.1 \cdot 10^{-4}$	–	1150 °C, 1 h	[39]
$\text{Li}_{6.16}\text{Al}_{0.28}\text{La}_3\text{Zr}_2\text{O}_{12}$	1 wt. % $\text{Li}_4\text{SiO}_4$	$6.1 \cdot 10^{-4}$	96.0	1200 °C	[40]
$\text{Li}_{6.16}\text{Al}_{0.28}\text{La}_3\text{Zr}_2\text{O}_{12}$	1 wt. % $\text{Li}_4\text{SiO}_4$	$4.1 \cdot 10^{-4}$	–	Hot pressing 1158 °C, 2 min	[41]
Al-doped $\text{Li}_7\text{La}_3\text{Zr}_2\text{O}_{12}$	3 wt. % $\text{Li}_2\text{O}-\text{Al}_2\text{O}_3-\text{SiO}_2$	$4.26 \cdot 10^{-4}$	97.0	1150 °C, 15 h	[42]
Al-doped $\text{Li}_7\text{La}_3\text{Zr}_2\text{O}_{12}$	1 wt. % $\text{Li}_2\text{O}-\text{Y}_2\text{O}_3-\text{SiO}_2$	$2.8 \cdot 10^{-4}$	–	1200 °C, 1 h	[43]
Al-doped $\text{Li}_7\text{La}_3\text{Zr}_2\text{O}_{12}$	1 wt. % $\text{Li}_2\text{O}-\text{B}_2\text{O}_3-\text{SiO}_2$	$3.0 \cdot 10^{-4}$	–	1150 °C, 1 h	[44]
$\text{Li}_7\text{La}_3\text{ZrNbO}_{12}$	4 wt. % $\text{Li}_2\text{O}-\text{B}_2\text{O}_3-\text{SiO}_2-\text{CaO}-\text{Al}_2\text{O}_3$	$7.78 \cdot 10^{-5}$	85–90	900 °C, 10 h	[45]
$\text{Li}_7\text{La}_3\text{ZrNbO}_{12}$	4 wt. % $\text{BaO}-\text{B}_2\text{O}_3-\text{SiO}_2-\text{CaO}-\text{Al}_2\text{O}_3$	$\sim 2.52 \cdot 10^{-5}$	85–90	900 °C, 10 h	[45]

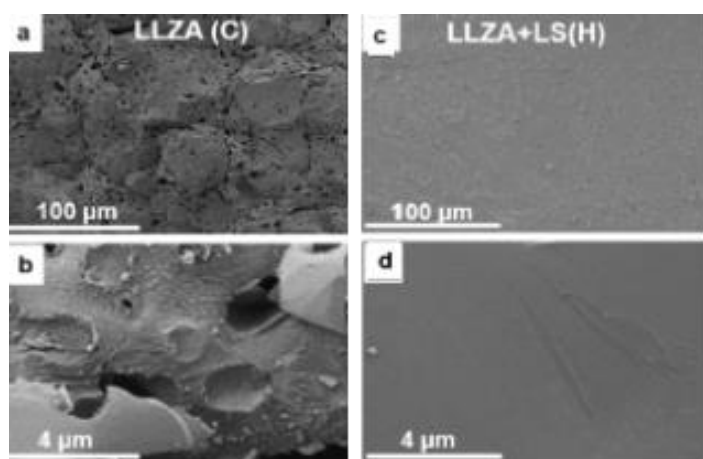


**Figure 3** Microphotographs of cross-sections of solid electrolyte  $\text{Li}_{6.16}\text{Al}_{0.28}\text{La}_3\text{Zr}_2\text{O}_{12}$  (a, b) and composite electrolyte  $\text{Li}_{6.16}\text{Al}_{0.28}\text{La}_3\text{Zr}_2\text{O}_{12} + 1 \text{ wt. } \% \text{ Li}_4\text{SiO}_4$  (c, d). Reprinted with permission from [41]. Copyright 2020, American Chemical Society.

Multicomponent glasses were also considered as sintering additives:  $\text{Li}_2\text{O}-\text{Al}_2\text{O}_3-\text{SiO}_2$  [42],  $\text{Li}_2\text{O}-\text{Y}_2\text{O}_3-\text{SiO}_2$  [43],  $\text{Li}_2\text{O}-\text{B}_2\text{O}_3-\text{SiO}_2$  [44],  $\text{Li}_2\text{O}-\text{B}_2\text{O}_3-\text{SiO}_2-\text{CaO}-\text{Al}_2\text{O}_3$  (LBSCA) and  $\text{BaO}-\text{B}_2\text{O}_3-\text{SiO}_2-\text{CaO}-\text{Al}_2\text{O}_3$  (BBSCA) [45]. It is well known that multicomponent glasses have higher conductivity values than bipolar compositions. The total conductivity of LLZ ceramics with 3 wt. %  $\text{Li}_2\text{O}-\text{Al}_2\text{O}_3-\text{SiO}_2$  sintered at 1150 °C for 15 hours reached  $4.26 \cdot 10^{-4} \text{ S/cm}$  at room temperature [42]. Composite solid electrolytes based on Al-doped LLZ with 1 wt. % of  $\text{Li}_2\text{O}-\text{Y}_2\text{O}_3-\text{SiO}_2$  ( $\text{Li}_2\text{O}-\text{B}_2\text{O}_3-\text{SiO}_2$ ) after annealing at 1150 °C possess higher conductivity values than Al-doped LLZ –  $2.8 \cdot 10^{-4} \text{ S/cm}$  at room temperature [43, 44]. In [45], in order to reduce the grain boundary resistance of LLZ, multicomponent glasses  $\text{Li}_2\text{O}-\text{B}_2\text{O}_3-\text{SiO}_2-\text{CaO}-\text{Al}_2\text{O}_3$  and  $\text{BaO}-\text{B}_2\text{O}_3-\text{SiO}_2-\text{CaO}-\text{Al}_2\text{O}_3$  with a low softening point were used. The composite solid electrolyte with 4 wt. %  $\text{Li}_2\text{O}-\text{B}_2\text{O}_3-\text{SiO}_2-\text{CaO}-\text{Al}_2\text{O}_3$ , sintered at 900 °C for 10 h, had the highest lithium-ion conductivity –  $8 \cdot 10^{-5} \text{ S/cm}$  at 30 °C.

Table 1 summarizes the presented in the literature composite solid electrolytes based on cubic LLZ with various sintering additives. It can be concluded that to obtain highly conductive composite solid electrolytes based on cubic LLZ, it is sufficient to introduce a small amount of sintering additive followed by heat treatment at temperatures above 1000 °C, or by increasing the holding time (more than 20 h) at temperatures of 800–900 °C.

## 1.2. Effect of various sintering additives on LLZ stabilization to air components and lithium dendrite penetration

It was mentioned above; the transition to composite solid electrolytes may be one of the ways to solve the stability problem of highly conductive solid electrolytes with the garnet-like structure to the air components [19–21, 30, 31, 34]. In work Zhang LC et al. [34] it was shown that conductivity of solid electrolyte without  $\text{Li}_3\text{BO}_3$  addition decrease from  $2.83 \cdot 10^{-6}$  to  $3.03 \cdot 10^{-8} \text{ S/cm}$  after 4 days exposure to air while composite solid electrolytes with the  $\text{Li}_3\text{BO}_3$  addition possess more stable behavior – a decrease in conductivity occurred from  $1.33 \cdot 10^{-4}$  to  $7.54 \cdot 10^{-5} \text{ S/cm}$ . Solid electrolytes  $\text{Li}_7\text{La}_3\text{Zr}_{1.75}\text{Nb}_{0.25}\text{Al}_{0.1}\text{O}_{12}$  with no  $\text{Li}_3\text{BO}_3$  and 4 wt. %  $\text{Li}_3\text{BO}_3$  were examined over 120 h of air exposure [30]. It was established that after 72 h of air exposure the ionic conductivity of  $\text{Li}_7\text{La}_3\text{Zr}_{1.75}\text{Nb}_{0.25}\text{Al}_{0.1}\text{O}_{12}$  pellets fell to ~ 20 % while the composite solid electrolyte fell to ~ 60 %. The effectiveness of composite electrolyte creation was also noted in [41]. The appearance of lithium carbonate impurities on the surface of the composite solid electrolytes (with the addition of  $\text{Li}_4\text{SiO}_4$ ) after exposure to an air atmosphere was not detected. The use of boron nitride (BN) as sintering additive was proposed as a promising solution to remove lithium carbonate from the surface of  $\text{Li}_{6.25}\text{Ga}_{0.25}\text{La}_3\text{Zr}_2\text{O}_{12}$  ceramic grains by Zhao G et al. [31]. During sintering, BN interacts with  $\text{Li}_2\text{CO}_3$  to form the  $\text{Li}_3\text{BO}_3$  phase, which, as mentioned, leads to the protection of LLZ from further interaction with air components.

In [43], a composite solid electrolyte with 1 wt. %  $\text{Li}_2\text{O}-\text{Y}_2\text{O}_3-\text{SiO}_2$  glass was kept in contact with air atmosphere for 30 days. The lithium-ion conductivity of Al-doped LLZ decreased significantly (from  $1.5 \cdot 10^{-4}$  to  $4.0 \cdot 10^{-6} \text{ S/cm}$  at room temperature) after exposure to air and was accompanied by an increase in the activation energy of conductivity. While exposure in air of the composite solid electrolyte leads to only a slight drop in lithium-ion conductivity (from  $2.8 \cdot 10^{-4}$  to  $1.5 \cdot 10^{-4} \text{ S/cm}$  at room temperature) without changing the activation energy of conductivity. It should be noted that the observed decrease in conductivity is significantly less than for the composite with the addition of  $\text{Li}_3\text{BO}_3$ , exposed to air for 4 days [34]. Thus, we can conclude that the addition of lithium-conductive glass to cubic LLZ increases the stability of the ceramic in contact with environmental components.

Another positive effect of the strategy of composite electrolyte formation is the increase in the ceramic wettability by Li and the way to prevent Li penetration

through the solid electrolyte. For example, the composite electrolyte based on LLZ with the addition of  $\text{Li}_4\text{SiO}_4$  [39] contributed to the formation of defect-free contact with Li, while the solid electrolyte without the additive had pores (defects) at the interface with Li anode (Figure 4). It was demonstrated in work [38] that the  $\text{Li}_3\text{PO}_4$  additive is concentrated along the grain boundaries of  $\text{Li}_{6.5}\text{La}_3\text{Zr}_{1.5}\text{Ta}_{0.5}\text{O}_{12}$ . Despite the fact that  $\text{Li}_{6.5}\text{La}_3\text{Zr}_{1.5}\text{Ta}_{0.5}\text{O}_{12}$  with the addition of 2 wt. %  $\text{Li}_3\text{PO}_4$  had lower conductivity values compared to the solid electrolyte without additive, this modification led to a decrease in the resistance at the solid electrolyte | Li interface from 2080 to  $1008 \Omega \cdot \text{cm}^2$  and suppresses the formation of Li dendrites in the studied symmetric cells during cycling. Modification of  $\text{Li}_{6.5}\text{La}_3\text{Zr}_{1.5}\text{Ta}_{0.5}\text{O}_{12}$  by introducing 2 wt. % LiOH leads to the filling of voids in the ceramic electrolyte and, as a consequence, to the suppression of the growth of lithium dendrites during the cycling of symmetric cells [22]. A composite solid electrolyte based on Ga-doped LLZ with the addition of 2 wt. % BN also contributed to the formation of a continuous coating with lithium metal and a decrease in the resistance of symmetric cells from 1219 to  $32 \Omega \cdot \text{cm}^2$  [31]. The decrease of interfacial resistance between the composite electrolyte ( $\text{Li}_{6.75}\text{La}_3\text{Zr}_{1.75}\text{Ta}_{0.25}\text{O}_{12}$  – 2 wt. %  $\text{Li}_3\text{OCl}$ ) and lithium metal from 1850 to  $90 \Omega \cdot \text{cm}^2$  was observed in work [24]. It was established that  $\text{Li}_3\text{OCl}$  *in-situ* reacts with Li and forms a stable and dense interfacial layer.

It can be concluded that the introduction of sintering additives in solid electrolytes based on cubic LLZ has a number of positive effects (Figure 5). However, it should be taken into account that the amount of the introduced additive has a significant effect on the resistance of the composite electrolyte and Li dendrites penetration [24, 32]. For example, in [32], the composite  $\text{Li}_{6.55}\text{La}_3\text{Zr}_{1.55}\text{Ta}_{0.45}\text{O}_{12}$  with 20 vol % (8.9 wt. %)  $\text{Li}_{2.3}\text{Co}_7\text{B}_{0.3}\text{O}_3$  additive showed stable behavior during cycling, while the introduction of 50 vol % (28 wt. %) additive leads to the penetration of Li dendrites through the solid electrolyte. Thus, it is important that the additive introduced into LLZ does not degrade in contact with Li anode during cycling. Moreover, sintering additives should have high values of lithium-ion conductivity. It was established using the method of distribution of relaxation times (DRT) to analyze the impedance plots of composite solid electrolytes based on LLZ that in the composite solid electrolyte the transport of lithium ions occurs along the grains of LLZ ceramics and the volume of additive replacing the pores [46].

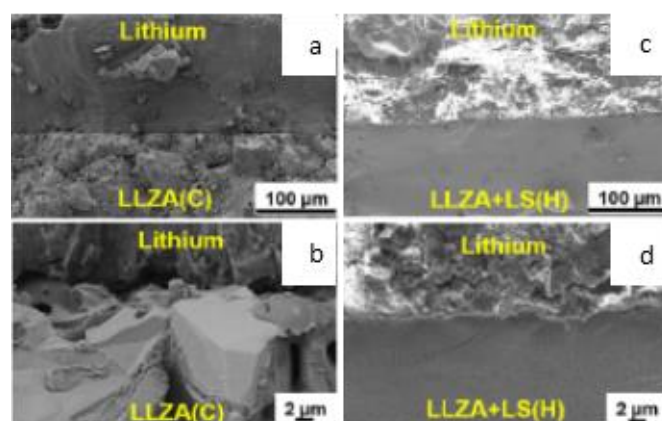


**Figure 4** Microphotographs of cross-sections of interface between Li and  $\text{Li}_{6.16}\text{Al}_{0.28}\text{La}_3\text{Zr}_2\text{O}_{12}$  (a, b) and  $\text{Li}_{6.16}\text{Al}_{0.28}\text{La}_3\text{Zr}_2\text{O}_{12} + 1 \text{ wt. } \% \text{ Li}_4\text{SiO}_4$  composite electrolyte (c, d). Reprinted with permission from [41]. Copyright 2020, American Chemical Society.

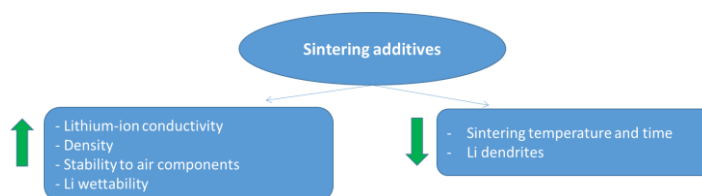


**Figure 5** The influence of the introduction of sintering additives on the properties and conditions of heat treatment of solid electrolytes based on LLZ.

## 2. Conclusions

The creation of composite solid electrolytes based on lithium-conducting solid electrolytes of the LLZ family is a promising area of research aimed at simultaneously solving a set of problems faced in the development of lithium all-solid-state power sources. The introduction of sintering additives into a ceramic electrolyte makes it possible to obtain high-density electrolyte membranes with high values of lithium-ion conductivity, increased stability to environmental components and resistance to lithium dendrite penetration.

However, the sintering additive had to meet the following requirements:

- low softening temperatures;
- high values of lithium-ion conductivity;
- stability in contact with lithium metal;
- absence of chemical interaction between components leading to the formation of low-conductivity impurity phases.

From the literature data, it can be concluded that to obtain highly conductive composite solid electrolytes based on LLZ it is necessary to introduce a small amount of sintering additive and then anneal at temperatures above  $1000 \text{ }^\circ\text{C}$ , or increase the holding time at lower temperatures.

The evolution of the developed direction of composite solid electrolyte starts from the introduction of one additive to ceramic then turn to two components addition, further progress has been achieved during the proposed technique of liquid-phase sintering from precursors of powder sintering additives prepared in the form of a solution. More suitable sintering additives:

- low-temperature lithium-ion compounds that modify grain boundaries together with the  $\text{Al}_2\text{O}_3$  additive that modifies the bulk of ceramic grains;
- multicomponent lithium-ion glasses that can modify the bulk and grain boundaries of LLZ ceramics.

Moreover, the strategy for transition to composite solid electrolytes has shown its promise in creating thin films based on LLZ. Thus, composite solid electrolytes are becoming increasingly attractive for all-solid-state power sources.

## Supplementary materials

No supplementary materials are available.

## Funding

This work was supported by the Research Program No 122020100210–9 (IHTE UB RAS), Russian Academy of Sciences, Ural Branch, Russia.

## Acknowledgments

None.

## Author contributions

Evgeniya Il'ina: Conceptualization; Data curation; Writing – Original draft; Writing – Review & Editing; Formal Analysis; Software; Visualization.

## Conflict of interest

The authors declare no conflict of interest.

## Additional information

Author IDs:

Scopus ID [54782709600](https://orcid.org/0000-0003-1759-5234);

ORCID [0000-0003-1759-5234](https://orcid.org/0000-0003-1759-5234).

## References

1. Guo Y, Wu S, He YB, Kang F, et al., Solid-state lithium batteries: Safety and prospects, *eScience*, **2** (2022) 138–163. <https://doi.org/10.1016/j.esci.2022.02.008>
2. Schreiber A, Rose, M, Waetzig K, Nikolowski K, et al., Oxide ceramic electrolytes for all-solid-state lithium batteries—Cost-cutting cell design and environmental impact, *Green*

- Chem., **25** (2023) 399–414. <https://doi.org/10.1039/D2GC03368B>
3. Mandade P, Weil M, Baumann M, Wei Z, Environmental life cycle assessment of emerging solid-state batteries: A review, *Chem. Engin. J. Adv.*, **13** (2023) 100439. <https://doi.org/10.1016/j.cej.2022.100439>
4. Bubulinca C, Kazantseva NE, Pechancova V, Joseph N, et al., Development of all-solid-state Li-Ion batteries: from key technical areas to commercial use, *Batteries*, **9** (2023) 157. <https://doi.org/10.3390/batteries9030157>
5. Chen L, Huang YF, Ma J, Ling H, et al., Progress and perspective of all-solid-state lithium batteries with high performance at room temperature, *En. Fuels*, **34** (2020) 13456–13472. <https://doi.org/10.1021/acs.energyfuels.0c02915>
6. Xu L, Li J, Deng W, Shuai H, et al., Garnet solid electrolyte for advanced all-solid-state Li batteries, *Adv. Energy Mater.*, **11** (2021) 2000648. <https://doi.org/10.1002/aenm.202000648>
7. Campanella D, Belanger D, Paoletta A, Beyond garnets, phosphates and phosphosulfides solid electrolytes: New ceramic perspectives for all solid lithium metal batteries, *J. Power Sources*, **482** (2021) 228949. <https://doi.org/10.1016/j.jpowsour.2020.228949>
8. Han Y, Chen Y, Huang Y, Zhang M, et al., Recent progress on garnet-type oxide electrolytes for all-solid-state lithium-ion batteries, *Ceram. Inter.*, **49** (2023) 29375–29390. <https://doi.org/10.1016/j.ceramint.2023.06.153>
9. Ramakumar S, Deviannapoorani C, Dhivya L, Shankar LS, et al., Lithium garnets: Synthesis, structure,  $\text{Li}^+$  conductivity,  $\text{Li}^+$  dynamics and applications, *Prog. Mater. Sci.*, **88** (2017) 325–411. <https://doi.org/10.1016/j.pmatsci.2017.04.007>
10. Il'ina E, Recent Strategies for Lithium-ion Conductivity Improvement in  $\text{Li}_7\text{La}_3\text{Zr}_2\text{O}_{12}$  Solid Electrolytes, *Int. J. Mol. Sci.*, **24(16)** (2023) 12905. <https://doi.org/10.3390/iims241612905>
11. Zhao J, Wang X, Wei T, Zhang Z, et al., Current challenges and perspectives of garnet-based solid-state electrolytes, *J. En. Stor.*, **68** (2023) 107693. <https://doi.org/10.1016/j.est.2023.107693>
12. Il'ina EA, Pershina SV, Composite Electrolytes Based on Tetragonal  $\text{Li}_7\text{La}_3\text{Zr}_2\text{O}_{12}$  for Lithium Batteries, Murugan R., Weppner W. (eds) *Solid Electrolytes for Advanced Applications*. Springer, Cham., 2019. [https://doi.org/10.1007/978-3-030-31581-8\\_8](https://doi.org/10.1007/978-3-030-31581-8_8)
13. Rosero-Navarro NC, Tadanaga K, Sintering Additives for Garnet-Type Electrolytes, Murugan R., Weppner W. (eds) *Solid Electrolytes for Advanced Applications*. Springer, Cham., 2019. [https://doi.org/10.1007/978-3-030-31581-8\\_5](https://doi.org/10.1007/978-3-030-31581-8_5)
14. Xie H, Feng, Zhao H, Lithium metal batteries with all-solid/full-liquid configurations, *En. Stor. Mater.*, **61** (2023) 102918. <https://doi.org/10.1016/j.ensm.2023.102918>
15. Chen Y, Qian J, Li L, Wu F et al., Advances in inorganic solid-state electrolyte/Li interface, *Chem. – A Europ. J.*, **30(5)** (2024) e202303454. <https://doi.org/10.1002/chem.202303454>
16. Wang J, Chen L, Li H, Wu F, et al., The anode interfacial issues in solid-state Li batteries: mechanistic understanding and mitigating strategies, *En. Envir. Mater.*, **6** (2023) e12613. <https://doi.org/10.1002/eem2.12613>
17. Cao D, Sun X, Li Q, Natan A, et al., Lithium dendrite in all-solid-state batteries: growth mechanisms, suppression

strategies, and characterizations, *Matter.*, **2** (2020) 1–38. <https://doi.org/10.1016/j.matt.2020.03.015>

18. Duan H, Zheng H, Zhou Y, Xu B, et al., Stability of garnet-type Li ion conductors: An overview, *Solid State Ion.*, **318** (2018) 45–53. <https://doi.org/10.1016/j.ssi.2017.09.018>

19. Hofstetter K, Samson AJ, Narayanan S, Thangadurai V, Present understanding of the stability of Li-stuffed garnets with moisture, carbon dioxide, and metallic lithium, *J. Power Sources*, **390** (2018) 297–312. <https://doi.org/10.1016/j.jpowsour.2018.04.016>

20. Ye R, Ihrig M, Imanishi N, Finsterbusch M, et al., A review on Li<sup>+</sup>/H<sup>+</sup> exchange in garnet solid electrolytes: from instability against humidity to sustainable processing in water, *ChemSusChem.*, **14** (2021) 4397–4407. <https://doi.org/10.1002/cssc.202101178>

21. Nakayama M, Horie T, Natsume R, Hashimura S, et al., Reaction kinetics of carbonation at the surface of garnet-type Li<sub>7</sub>La<sub>3</sub>Zr<sub>2</sub>O<sub>12</sub> as solid electrolytes for all-solid-state li ion batteries, *J. Phys. Chem. C.*, **127** (2023) 7595–760. <https://doi.org/10.1021/acs.jpcc.2c08588>

22. Basappa RH, Ito T, Morimura T, Bekarevich R, et al., Grain boundary modification to suppress lithium penetration through garnet-type solid electrolyte, *J. Power Sources*, **363** (2017) 145–152. <https://doi.org/10.1016/j.jpowsour.2017.07.088>

23. Hao S, Zhang H, Yao W, Lin J, Solid-state lithium battery chemistries achieving high cycle performance at room temperature by a new garnet-based composite electrolyte, *J. Power Sources*, **393** (2018) 128–134. <https://doi.org/10.1016/j.jpowsour.2018.05.028>

24. Tian Y, Ding F, Zhong H, Liu C, et al., Li<sub>6.75</sub>La<sub>3</sub>Zr<sub>1.75</sub>Ta<sub>0.25</sub>O<sub>12</sub>@amorphous Li<sub>3</sub>OCl composite electrolyte for solid state lithium-metal batteries, *En. Stor. Mater.*, **14** (2018) 49–57. <https://doi.org/10.1016/j.ensm.2018.02.015>

25. Ferreira EB, Lima ML, Zanotto ED, DSC method for determining the liquidus temperature of glass-forming systems, *J. Am. Ceram. Soc.*, **93** (2010) 3757–3763. <https://doi.org/10.1111/j.1551-2916.2010.03976.x>

26. Shin RH, Son S, Han YS, Kim YD et al., Sintering behavior of garnet-type Li<sub>7</sub>La<sub>3</sub>Zr<sub>2</sub>O<sub>12</sub>-Li<sub>3</sub>BO<sub>3</sub> composite solid electrolytes for all-solid-state lithium batteries, *Solid State Ion.*, **301** (2017) 10–14. <https://doi.org/10.1016/j.ssi.2017.01.005>

27. Takano R, Tadanaga K, Hayashi A, Tatsumisago M, Low temperature synthesis of Al-doped Li<sub>7</sub>La<sub>3</sub>Zr<sub>2</sub>O<sub>12</sub> solid electrolyte by a sol-gel process, *Solid State Ion.*, **255** (2014) 104–107. <https://doi.org/10.1016/j.ssi.2013.12.006>

28. Rosero-Navarro NC, Yamashita T, Miura A, Higuchi M, et al., Preparation of Li<sub>7</sub>La<sub>3</sub>(Zr<sub>2-x</sub>Nb<sub>x</sub>)O<sub>12</sub> (x = 0–1.5) and Li<sub>3</sub>BO<sub>3</sub>/LiBO<sub>2</sub> composites at low temperatures using a sol-gel process, *Solid State Ion.*, **285** (2016) 6–12. <https://doi.org/10.1016/j.ssi.2015.06.015>

29. Tadanaga K, Takano R, Ichinose T, Mori S, et al., Low temperature synthesis of highly ion conductive Li<sub>7</sub>La<sub>3</sub>Zr<sub>2</sub>O<sub>12</sub>-Li<sub>3</sub>BO<sub>3</sub> composites, *Electrochem. Commun.*, **33** (2013) 51–54. <https://doi.org/10.1016/j.elecom.2013.04.004>

30. Jonson RA, McGinn PJ, Tape casting and sintering of Li<sub>7</sub>La<sub>3</sub>Zr<sub>1.75</sub>Nb<sub>0.25</sub>Al<sub>0.1</sub>O<sub>12</sub> with Li<sub>3</sub>BO<sub>3</sub> additions, *Solid State Ion.*, **323** (2018) 49–55. <https://doi.org/10.1016/j.ssi.2018.05.015>

31. Zhao G, Luo C, Hua Q, Enhanced comprehensive performance of the LLZO series solid electrolyte via

multifunctional additive, *J. Europ. Ceram. Soc.*, **44(4)** (2024) 2251–2260.

<https://doi.org/10.1016/j.jeurceramsoc.2023.11.045>

32. Hosokawa H, Takeda A, Inada R, Sakurai Y, Tolerance for Li dendrite penetration in Ta-doped Li<sub>7</sub>La<sub>3</sub>Zr<sub>2</sub>O<sub>12</sub> solid electrolytes sintered with Li<sub>2.3</sub>Co<sub>0.7</sub>Bo<sub>0.3</sub>O<sub>3</sub> additive, *Mater. Lett.*, **279** (2020) 128481.

<https://doi.org/10.1016/j.matlet.2020.128481>

33. Rosero-Navarro NC, Miura A, Higuchi M, Tadanaga K, Optimization of Al<sub>2</sub>O<sub>3</sub> and Li<sub>3</sub>BO<sub>3</sub> content as sintering additives of Li<sub>7-x</sub>La<sub>2.95</sub>Ca<sub>0.05</sub>ZrTaO<sub>12</sub> at low temperature, *J. Electronic. Mater.*, **46** (2017) 497–501.

<https://doi.org/10.1007/s11664-016-4924-4>

34. Zhang LC, Yang JF, Gao YX, Wang XP, et al., Influence of Li<sub>3</sub>BO<sub>3</sub> additives on the Li<sup>+</sup> conductivity and stability of Ca/Ta-substituted Li<sub>6.55</sub>(La<sub>2.95</sub>Ca<sub>0.05</sub>)(Zr<sub>1.5</sub>Ta<sub>0.5</sub>)O<sub>12</sub> electrolytes, *J. Power Sources*, **355** (2017) 69–73.

<http://dx.doi.org/10.1016/j.jpowsour.2017.04.0440378-7>

35. Hayashi N, Watanabe K, Shimano K, Co-sintering a cathode material and garnet electrolyte to develop a bulk-type solid-state Li metal battery with wide electrochemical windows, *J. Mater. Chem.*, **A12** (2024) 5269–5281.

<https://doi.org/10.1039/D3TA06747E>

36. Rosero-Navarro NC, Watanabe H, Miura A, Tadanaga K, Synthesis of highly Li-ion conductive garnet-type solid ceramic electrolytes by solution-process-derived sintering additives, *J. Europ. Ceram. Soc.*, **41(13)** (2021) 6767–6771.

<https://doi.org/10.1016/j.jeurceramsoc.2021.06.045>

37. Yang C, Yi-Qiu L, Xiang-Xin G, Densification and lithium ion conductivity of garnet type Li<sub>7-x</sub>La<sub>3</sub>Zr<sub>2-x</sub>Ta<sub>x</sub>O<sub>12</sub> (x = 0.25) solid electrolytes, *Chin. Phys. B.*, **22** (2013) 0782011–0782015. <https://doi.org/10.1088/1674-1056/22/7/078201>

38. Xu B, Li W, Duan H, Wang H, et al., Li<sub>3</sub>PO<sub>4</sub>-added garnet-type Li<sub>6.5</sub>La<sub>3</sub>Zr<sub>1.5</sub>Ta<sub>0.5</sub>O<sub>12</sub> for Li-dendrite suppression, *J. Power Sources*, **354** (2017) 68–73.

<https://doi.org/10.1016/j.jpowsour.2017.04.026>

39. Pershina SV, Il'ina EA, Reznitskikh OG, Phase composition, density and ionic conductivity of the Li<sub>7</sub>La<sub>3</sub>Zr<sub>2</sub>O<sub>12</sub>-based composites with LiPO<sub>3</sub> glass addition, *Inorg. Chem.*, **56(16)** (2017) 9880–9891.

<https://doi.org/10.1021/acs.inorgchem.7b01379>

40. Janani N, Deviannapoorani C, Dhivya L, Murugan R, Influence of sintering additives on densification and Li<sup>+</sup> conductivity of Al doped Li<sub>7</sub>La<sub>3</sub>Zr<sub>2</sub>O<sub>12</sub> lithium garnet, *RSC Adv.*, **4** (2014) 51228–51238.

<https://doi.org/10.1039/C4RA08674K>

41. Patra S, Narayanasamy J, Chakravarty S, Murugan R, Higher critical current density in lithium garnets at room temperature by incorporation of an Li<sub>4</sub>SiO<sub>4</sub>-related glassy phase and hot isostatic pressing, *ACS Appl. Energy Mater.*, **3** (2020) 2737–743. <https://dx.doi.org/10.1021/acs.aem.9b02400>

42. Tang Y, Zhang Q, Luo Z, Liu P, et al., Effects of Li<sub>2</sub>O-Al<sub>2</sub>O<sub>3</sub>-SiO<sub>2</sub> system glass on the microstructure and ionic conductivity of Li<sub>7</sub>La<sub>3</sub>Zr<sub>2</sub>O<sub>12</sub> solid electrolyte, *Mater. Lett.*, **193** (2017) 251–254. <https://doi.org/10.1016/j.matlet.2017.01.134>

43. Il'ina EA, Druzhinin KV, Antonov BD, Pankratov AA, et al., Influence of Li<sub>2</sub>O-Y<sub>2</sub>O<sub>3</sub>-SiO<sub>2</sub> glass additive on conductivity and stability of cubic Li<sub>7</sub>La<sub>3</sub>Zr<sub>2</sub>O<sub>12</sub>, *Ionics*, **25(11)** (2019) 5189–5199. <https://doi.org/10.1007/s11581-019-03077-3>



44. Il'ina EA, Pershina SV, Antonov BD, Pankratov AA, et al., The influence of the glass additive  $\text{Li}_2\text{O}-\text{B}_2\text{O}_3-\text{SiO}_2$  on the phase composition, conductivity, and microstructure of the  $\text{Li}_7\text{La}_3\text{Zr}_2\text{O}_{12}$ , J. All. Comp., **765** (2018) 841–847. <https://doi.org/10.1016/j.jallcom.2018.06.154>

45. Rosero-Navarro NC, Yamashita T, Miura A, Higuchi M, et al., Effect of sintering additives on relative density and Li-ion conductivity of Nb-doped  $\text{Li}_7\text{La}_3\text{Zr}_2\text{O}_{12}$  solid electrolyte, J. Am. Ceram. Soc., **100** (2016) 276–285. <https://doi.org/10.1111/jace.145>

46. Il'ina E, Osinkin D, Interpretation of the resistance of  $\text{Li}_7\text{La}_3\text{Zr}_2\text{O}_{12} - \text{Li}_2\text{O}-\text{B}_2\text{O}_3-\text{SiO}_2$  composite electrolytes for all-solid-state batteries using the distribution of relaxation times technique, J. Power Sources, **580** (2023) 233370. <https://doi.org/10.1016/j.jpowsour.2023.233370>